NUMERICAL SIMULATION ON EVALUATING CALIBRATION RESULTS OF NON-METRIC DIGITAL CAMERA

Ryuji Matsuoka*, Kiyonari Fukue, Kohei Cho, Haruhisa Shimoda, Yoshiaki Matsumae

Tokai University Research & Information Center
2-28-4 Tomigaya, Shibuya-ku, Tokyo 151-0063, JAPAN
ryuji@yoyogi.ycc.u-tokai.ac.jp, fku@keyaki.cc.u-tokai.ac.jp, kcho@keyaki.cc.u-tokai.ac.jp,
smd@keyaki.cc.u-tokai.ac.jp, jjm@keyaki.cc.u-tokai.ac.jp

KEY WORDS: Digital, Calibration, Orientation, Simulation, Camera, Distortion, Non-Metric, Method

ABSTRACT:

A non-metric digital camera is required to be geometrically calibrated when it is used for photogrammetric applications. Many camera calibration methods for a non-metric digital camera have been proposed. However there is no standard procedure to evaluate an estimated image distortion model directly. Calibration results are usually evaluated indirectly by such indexes as residuals on image, three-dimensional measurement errors of control points, and error estimates of obtained camera parameters. Therefore, we conducted a numerical simulation in order to examine capabilities of these indexes. In the simulation nine images were supposed to be acquired vertically to shoot 1024 control points on four layers disposed at regular intervals of the depth. Seven sets of 1024 control points were prepared, and these sets varied in the depth of the distribution of control points from 2/3 to 1/96 of the average camera height. In the simulation 49 cases with different sets of control points and different precision of image coordinates were investigated. Numerical simulation results show the limits of capabilities of these indexes. A larger value of one of these indexes obtained in a camera calibration usually means that the image distortion model estimated by the calibration is not reasonable. On the other hand, smaller values of all of these indexes do not always mean that the estimated image distortion model is appropriate. Thus the authors propose that a set of the prior and posterior numerical simulations should be conducted in a camera calibration to evaluate calibration results in addition to conventional evaluation by using the abovementioned indexes.

1. INTRODUCTION

As performance of a digital camera becomes better and its price becomes lower in the last several years, digital camera images are becoming more popular in diverse fields. The recent increase in number of pixels of acquired images encourages an amateur to utilize a non-metric digital camera for photogrammetric applications such as three-dimensional measurements and creation of orthoimages.

A non-metric digital camera is required to be geometrically calibrated when it is used for photogrammetric applications. Many camera calibration methods for a non-metric digital camera have been proposed.

However, there is no standard procedure to evaluate the estimated image distortion model directly. Calibration results are usually evaluated indirectly by such indexes as residuals on image, three-dimensional measurement errors of control points, and error estimates of obtained camera parameters. Therefore we conducted a numerical simulation in order to investigate to what extent these indexes can indicate the reliability of the estimated image distortion model.

2. CURRENT CAMERA CALIBRATION

2.1 Calibration Methods of Non-Metric Cameras

There are several calibration methods of close range cameras (Fryer, 1996; Fraser, 2001). Laboratory calibration methods by using a multi-collimator or a goniometer are popular for metric cameras, but are rarely conducted for a non-metric camera owing to its higher cost. Field calibration methods including self-calibration are usually adopted for a non-metric camera.

In this paper, we focus on a field calibration method of a non-metric digital camera. Moreover, we define the aim of the camera calibration as estimating the image distortion model of images acquired by the target camera.

2.2 Evaluation of Calibration Results

Most of the image distortion models obtained by a field calibration are not evaluated directly. Calibration results are usually evaluated indirectly by some indexes such as (A) residuals on image, (B) three-dimensional measurement errors of control points, and (C) error estimates of obtained camera parameters.

As to calibration of a non-metric analog camera, Nasu (1980) used the indexes (A) and (C) to evaluate effectiveness of camera calibration. Murai *et al.* (1984) examined various sets of additional parameters using the indexes (A) and (B). Meanwhile as to calibration of a non-metric digital camera, Chikatsu *et al.* (1996) employed all indexes (A), (B) and (C) to evaluate experimental results of their proposed calibration method. Noma *et al.* (2002) demonstrated the performance of their developed calibration system with the indexes (A) and (B). Moreover Habib *et al.* (2002) utilized the indexes (A) and (C) to evaluate the feasibility of the suggested approach.

3. NUMERICAL SIMULATION

The numerical simulation was conducted in order to examine characteristics of the evaluation indexes of calibration results mentioned in the previous section. The reasons why we adopted the numerical simulation are as follows:
(1) To avoid mixture of unexpected image distortion.

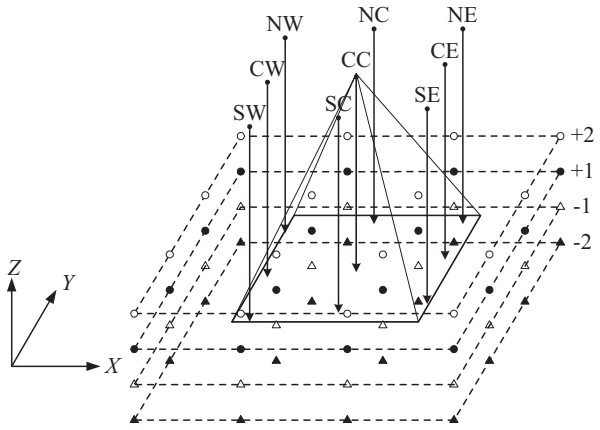

Figure 1. Image acquisition for the calibration

	Points	Set	Interval d (m)	Range D (m)	D_Z / H
X	16		0.320	4.800	
Y	16		0.320	4.800	
Z	4	Z-1	0.640	1.920	2/3
		Z-2	0.320	0.960	1/3
		Z-3	0.160	0.480	1/6
		Z-4	0.080	0.240	1/12
		Z-5	0.040	0.120	1/24
		Z-6	0.020	0.060	1/48
		Z-7	0.010	0.030	1/96

Table 1. Dispositions of control points

(2) To evaluate reproductivity of the image distortion model.
(3) To execute analysis independent of accuracy of ground coordinates of control points.
(4) To control precision of image coordinates.
(5) To reduce examination expenses.

3.1 Outline of the Numerical Simulation

Figure 1 shows a sketch of image acquisition for the calibration supposed in the numerical simulation. Three images by three images, nine images in all were supposed to be acquired vertically to shoot control points on four layers disposed in the depth. The reason why we adopted this calibration plan was that reliability of calibration results was expected to be controllable by the only factor, that is, the depth of the distribution of control points. A deeper distribution of control points would provide more reliable calibration results, on the other hand, calibration results obtained by using a shallower distribution of control points would be unreliable.

3.1.1 Control Points: We prepared seven sets [Z-1 ~ Z-7] of 1024 control points placed on four layers disposed at regular intervals of the depth (Z). Each layer had 16 points (X) by 16 points (Y) uniformly distributed control points. Sets of control points varied in the depth (D_Z) of the distribution of control points from 2/3 to 1/96 of the average camera height (H = 2.880 m.) Z coordinate of the distribution center of control points of each set [Z-1 ~ Z-7] was 0 m. Table 1 shows dispositions of control points.

3.1.2 Images: It was assumed that three images (X) [W, C, E] by three images (Y) [N, C, S], nine images in all were acquired vertically and each image had an approximately 50 % overlapping ratio of the adjacent images at Z = 0. Camera positions of the nine images were not uniformly distributed as shown in Table 2, since control points were uniformly distributed. The average camera height (H) of the nine images was 2.880 m. Figure 2 shows the coverage of each image at Z = 0.

	<W>	<C>	<E>
<N>	Image NW	Image NC	Image NE
	X_0 -1.040 m	X_0 -0.080 m	X_0 1.040 m
	Y_0 1.200 m	Y_0 1.120 m	Y_0 1.200 m
	Z_0 2.840 m	Z_0 2.920 m	Z_0 2.840 m
<C>	Image CW	Image CC	Image CE
	X_0 -1.120 m	X_0 0.000 m	X_0 1.120 m
	Y_0 0.080 m	Y_0 0.000 m	Y_0 -0.080 m
	Z_0 2.920 m	Z_0 2.880 m	Z_0 2.920 m
<S>	Image SW	Image SC	Image SE
	X_0 -1.040 m	X_0 0.080 m	X_0 1.040 m
	Y_0 -1.200 m	Y_0 -1.120 m	Y_0 -1.200 m
	Z_0 2.840 m	Z_0 2.920 m	Z_0 2.840 m

Table 2. Camera positions

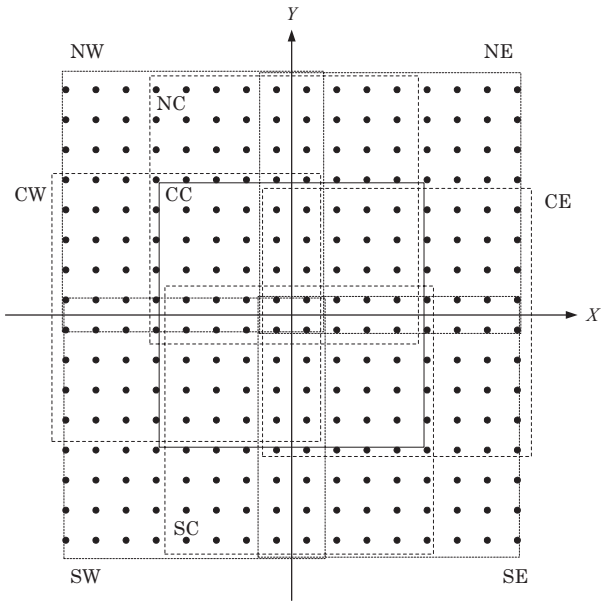

Figure 2. Coverage of each image at Z = 0

Random Gaussian errors with 1/3 pixels of standard deviation σ_0 ($3\sigma_0$ = 1 pixel) were added to each image coordinate of calibration points as for the standard datasets. Furthermore, random Gaussian errors with 1 pixel and 1/6 pixels of standard deviation σ_0 ($3\sigma_0$ = 3 pixels and $3\sigma_0$ = 1/2 pixels) were added to each image coordinate as for two additional reference datasets respectively.

3.1.3 Camera: The target camera assumed in the simulation had an image pickup element of 9 mm by 9 mm, and the focal length of its lens was 9 mm (equivalent to 35 mm in 35 mm film format). An image acquired by the target camera was recorded as a 2250 pixels by 2250 pixels image. Hence, the interval between pixels was 4.0 μm.

Image distortion (Δx, Δy) of a point (x, y) is represented as

			Setup values
Offsets of the principal point	x_p	(pixel)	20.00
	y_p	(pixel)	-20.00
Principal distance	c	(mm)	9.225
Radial distortion	k_1	(mm^{-2})	2.0000000×10^{-3}
	k_2	(mm^{-4})	-1.5000000×10^{-5}
	k_3	(mm^{-6})	-2.0000000×10^{-7}
Decentering distortion	p_1	(mm^{-1})	1.0000000×10^{-4}
	p_2	(mm^{-1})	-1.0000000×10^{-4}

Table 3. Setup values of the image distortion model

$$\begin{cases} \Delta x = x_p + \left(\dfrac{\Delta c}{c_0}\right)\overline{x} + \overline{x}\left(k_1 r^2 + k_2 r^4 + k_3 r^6\right) \\ \quad + p_1\left(r^2 + 2\overline{x}^2\right) + 2p_2\overline{xy} \\ \Delta y = y_p + \left(\dfrac{\Delta c}{c_0}\right)\overline{y} + \overline{y}\left(k_1 r^2 + k_2 r^4 + k_3 r^6\right) \\ \quad + 2p_1\overline{xy} + p_2\left(r^2 + 2\overline{y}^2\right) \end{cases} \tag{1}$$

$$\begin{cases} r^2 = \overline{x}^2 + \overline{y}^2 \\ \overline{x} = x - x_p \\ \overline{y} = y - y_p \end{cases} \tag{2}$$

where x_p, y_p are the offsets from the principal point to the center of the image frame, Δc is the correction to the assumed principal distance c_0, and k_1, k_2, k_3 are the coefficients of radial distortion, p_1, p_2 are the coefficients of decentering distortion.

Setup values of the image distortion model are shown in Table 3. These values were based on experimental results of the calibration of an Olympus CAMEDIA E-10 (Matsuoka *et al.* 2002). Its image pickup element is 2/3-inch type CCD (4 million pixels total; 3.9 million pixels effective), and its lens is 9 - 36 mm (equivalent to 35 - 140 mm zoom in 35 mm film format) Olympus lens. A 2240 pixels by 1680 pixels image is acquired at the maximum resolution with the 3.9 μm interval between pixels.

3.1.4 Experimental Cases: 1024 control points in each set were divided into four groups [P ~ S] so that each group had four layers of 64 control points per layer. A standard case of camera calibration in the simulation employed one group of 256 control points, consequently four cases [P ~ S] by seven sets [Z-1 ~ Z-7], 28 standard cases in total were executed in the simulation.

In addition to the standard cases, three reference cases [T-1, T-3, T-6] for each set [Z-1 ~ Z-7] were executed. Each reference case employed all 1024 control points. Standard deviations of added image coordinate errors of the reference cases T-1, T-3, and T-6 were 1 pixel, 1/3 pixels and 1/6 pixels respectively. Table 4 shows numbers of control points and standard deviations of added image coordinate errors of seven experimental cases [P ~ S, T-1, T-3, T-6] for each set [Z-1 ~ Z-7].

Case		Number of control points	Std. dev. of added errors
standard	P	256	1/3
	Q	256	1/3
	R	256	1/3
	S	256	1/3
reference	T-1	1024	1/1
	T-3	1024	1/3
	T-6	1024	1/6

Table 4. Experimental cases for each set [Z-1 ~ Z-7]

Difference of calibration results between the standard case [P ~ S] and the reference case T-3 would indicate the influence of the number of control points. Furthermore, difference of calibration results between the reference cases T-1, T-3, and T-6 would indicate the influence of the measurement precision of image coordinates.

3.1.5 Evaluation Indexes: The following evaluation indexes were examined in the simulation:

(A) Residuals on image calculated at the calibration
(B) Three-dimensional measurement errors of control points calculated at the calibration
(C) Error estimates of obtained camera parameters calculated at the calibration
(D) Three-dimensional measurement errors of control points calculated at the posterior three-dimensional measurement using the obtained image distortion model. Positions and attitudes of the camera used at the posterior three-dimensional measurement were unknown and estimated by an orientation. The posterior orientation was executed using the different set of control points from that used at the calibration.
(E) Three-dimensional measurement errors of control points calculated at the posterior three-dimensional measurement using the obtained image distortion model. Positions and attitudes of the camera used at the posterior three-dimensional measurement were given. No orientation for the posterior three-dimensional measurement was carried out.
(F) Differences of image distortions calculated at all pixels on the image between the obtained image distortion model and the setup one

The indexes (D) and (E) are not evaluated in an ordinary camera calibration. The index (F) is an ideal index to evaluate an obtained image distortion model in a camera calibration, but it can be calculated only in a numerical simulation.

3.2 Results and Discussion

3.2.1 Results: Figures 3 to 11 show values of the abovementioned evaluation indexes obtained in the simulation. As for the standard cases [P ~ S], the line graph shows the mean values of four cases, and the maximum and minimum values are illustrated as error bars in all these figures. Values of the indexes (A), (B) and (C) obtained by the reference cases [T-1, T-3, T-6] are illustrated in Figures 3, and 5 to 8 respectively.

(A) Figure 3 shows the root mean squares V_P of residuals on image calculated at the calibration. Since the dispersion among the four standard cases [P ~ S] was very small, the error bars of the maximum and minimum values become unrecognizable.

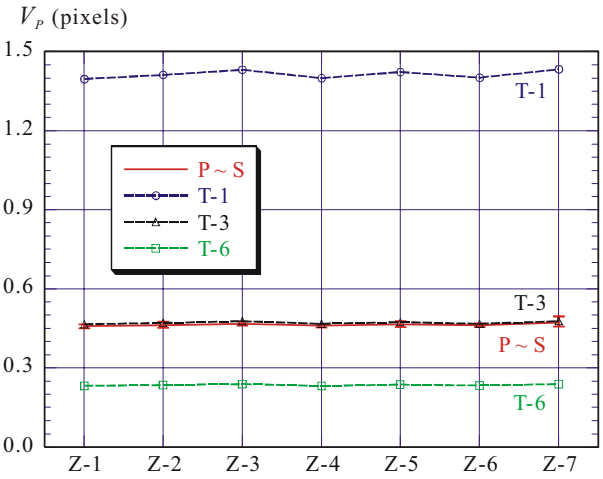

Figure 3. (A) Root mean squares V_P of residuals on image

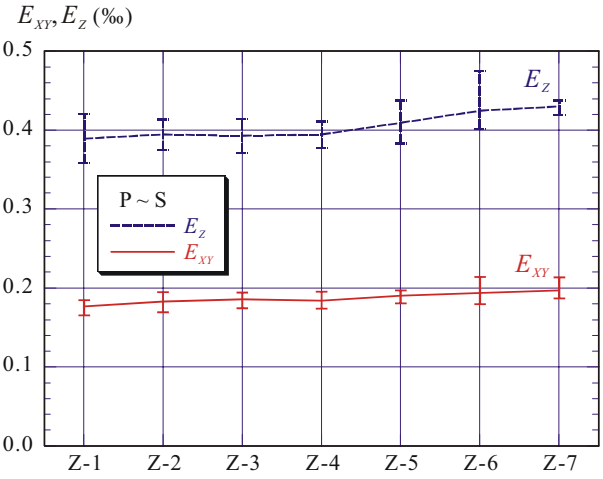

Figure 4. (B) Three-dimensional measurement errors E_{XY}, E_Z

(B) Figures 4, 5 and 6 show the three-dimensional measurement errors E_{XY} and E_Z of control points calculated at the calibration. E_{XY} and E_Z are the standard deviations of horizontal and vertical relative errors respectively, and were calculated using the following equation:

$$\begin{cases} E_{XY} = \sqrt{\dfrac{1}{n}\sum_{i=1}^{n}\left\{\dfrac{\left(e_{Xi}^2 + e_{Yi}^2\right)^{1/2}}{H - Z_i}\right\}^2} \\ E_Z = \sqrt{\dfrac{1}{n}\sum_{i=1}^{n}\left(\dfrac{e_{Zi}}{H - Z_i}\right)^2} \end{cases} \tag{3}$$

where (e_{Xi}, e_{Yi}, e_{Zi}) is the three-dimensional measurement error of the control point $i\,(X_i, Y_i, Z_i)$, n is the number of control points, and H is the average camera height of the nine images.

The unit ‰ (per mill) in Figures 4, 5 and 6 means 10^{-3}.

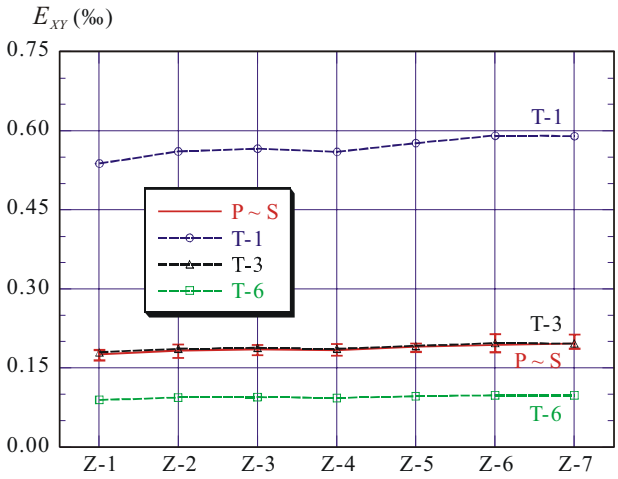

Figure 5. (B) Three-dimensional measurement errors: Horizontal relative errors E_{XY}

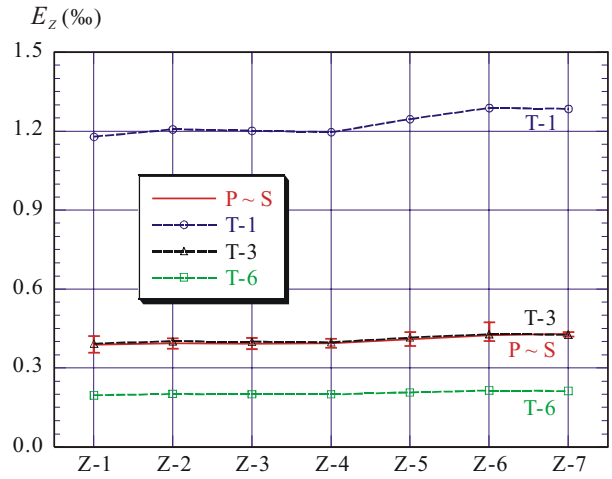

Figure 6. (B) Three-dimensional measurement errors: Vertical relative errors E_Z

(C) Figure 7 shows the error estimate σ_c of the obtained principal distance and Figure 8 shows the error estimate σ_p of the obtained offset of the principal point. σ_p was calculated using the following equation:

$$\sigma_p = \sqrt{\sigma_{xp}^2 + \sigma_{yp}^2} \tag{4}$$

where $(\sigma_{xp}, \sigma_{yp})$ is the error estimate of the offset (x_p, y_p) from the principal point to the center of the image frame.

As for sets [Z-1 ~ Z-4] of deeper distributions of control points, since the dispersions of both σ_c and σ_p among the four standard cases [P ~ S] were very small, the error bars of the maximum and minimum values of both σ_c and σ_p become unrecognizable.

(D) Figure 9 shows three-dimensional measurement errors E_{XY} and E_Z of control points at the posterior three-dimensional

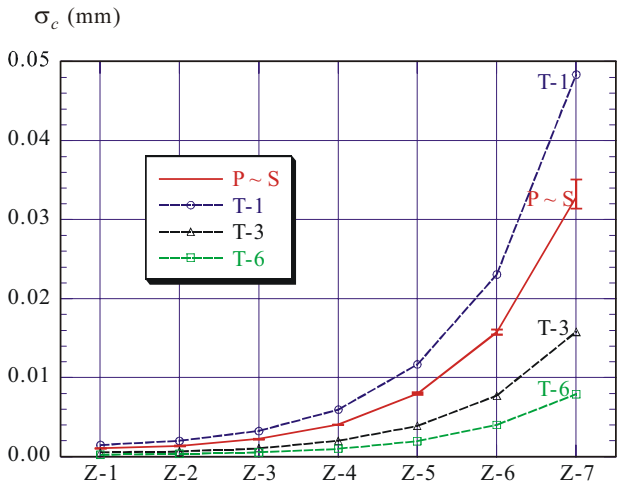

Figure 7. (C) Error estimate σ_c of the obtained principal distance

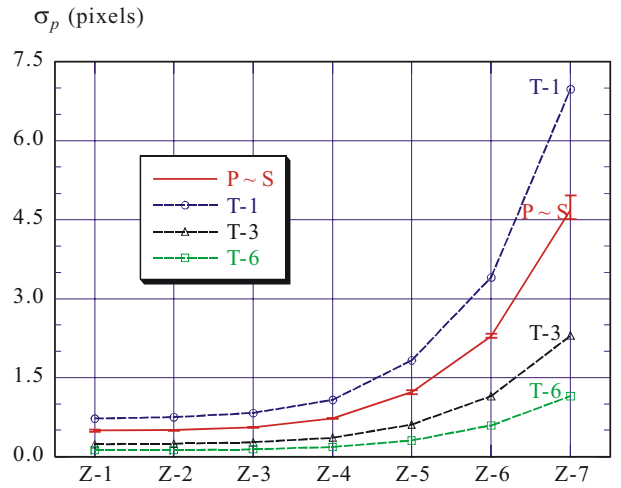

Figure 8. (C) Error estimate σ_p of the obtained offset of the principal point

measurement with orientation. E_{XY} and E_Z are the standard deviations of horizontal and vertical relative errors respectively, and were calculated using the equation (3). The unit ‰ (per mill) in Figure 9 means 10^{-3}.

(E) Figure 10 shows three-dimensional measurement errors E_{XY} and E_Z of control points at the posterior three-dimensional measurement without orientation. E_{XY} and E_Z are the standard deviations of horizontal and vertical relative errors respectively, and were calculated using the equation (3) in the same way as Figure 9. The unit ‰ (per mill) in Figure 10 also means 10^{-3}.

(F) Figure 11 shows root mean squares D_T of differences of image distortions calculated at all pixels on the image. D_T was calculated using the following equation:

$$D_T = \sqrt{\frac{1}{N}\sum_{k=1}^{N}\left\{\left(\Delta x_k^{(T)} - \Delta x_k^{(S)}\right)^2 + \left(\Delta y_k^{(T)} - \Delta y_k^{(S)}\right)^2\right\}} \quad (5)$$

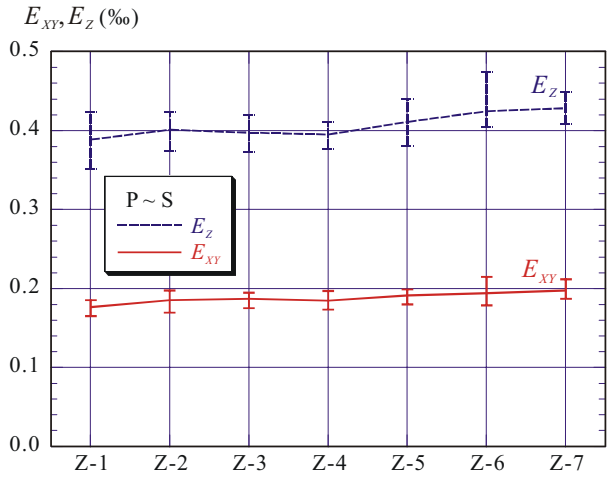

Figure 9. (D) Posterior three-dimensional measurement errors E_{XY}, E_Z with orientation

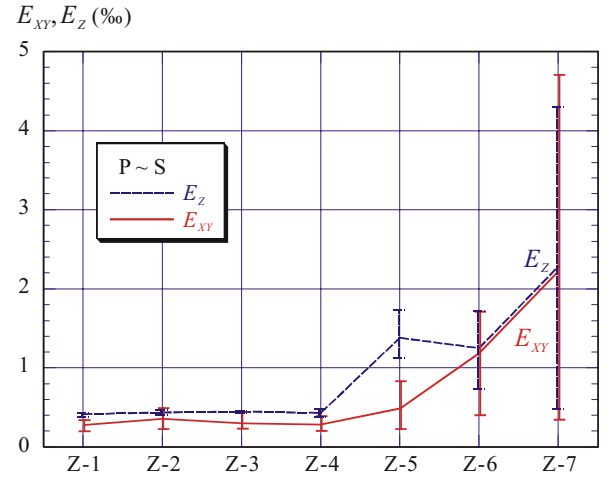

Figure 10. (E) Posterior three-dimensional measurement errors E_{XY}, E_Z without orientation

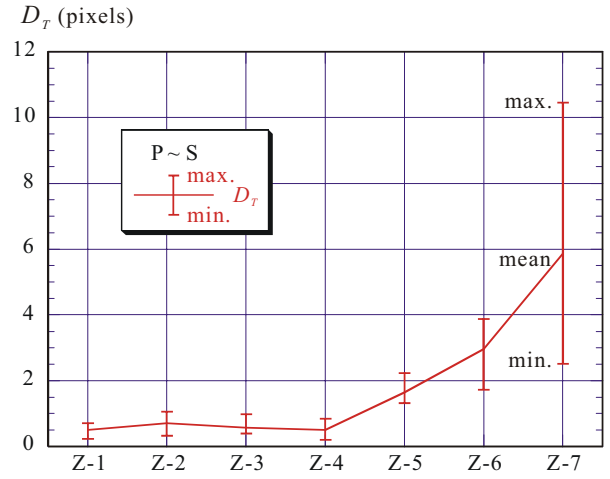

Figure 11. (F) Root mean squares D_T of differences of image distortions

where $\left(\Delta x_k^{(T)}, \Delta y_k^{(T)}\right)$ and $\left(\Delta x_k^{(S)}, \Delta y_k^{(S)}\right)$ are image distortions calculated at the pixel $k\left(x_k, y_k\right)$ by using the obtained image distortion model and the setup one respectively, and N is the number of pixels of the image. In the simulation, N was 5,062,500 (2250 by 2250).

3.2.2 Discussion: Image distortion models estimated by using sets of control points with the shallower distributions less than 1/20 of the camera height were judged inappropriate by values of the indexes (E) and (F) shown in Figures 10 and 11. In a word, a camera calibration resulted in failure in 12 cases [Z-5 ~ Z-7] out of all 28 standard cases.

All values of the index (A) calculated in 28 standard cases were practically the same as Figure 3 shows. Moreover, differences in the index (B) among all 28 standard cases were small as Figure 4 shows. No significant differences in the index (D) among all 28 standard cases shown in Figure 9 were observed as well. These results support the conclusion that the indexes (A), (B) and (D) cannot indicate the reliability of the estimated image distortion model.

Figures 3, 5 and 6 indicate that values of the indexes (A) and (B) were affected by the precision of the measurement of image coordinates, but not by the number of control points. Thus the indexes (A) and (B) can be utilized to evaluate the precision of observations in a camera calibration.

On the other hand, values of the index (C) varied in accordance with the depth of the distribution of control points as shown in Figures 7 and 8. The index (C) seems to be a promising index to evaluate camera calibration results.

Figures 7 and 8 show that a value of the index (C) was in proportion to the square root of the number of observations, namely, the square root of the number of control points used in the calibration. Furthermore, values of the index (C) were affected by the precision of the measurement of image coordinates. Therefore, it is very difficult to interpret absolute values of the index (C) obtained in a camera calibration. If one obtains the value 0.010 mm of the error estimate σ_c of the principal distance or the value 1.4 pixels of the error estimate σ_p of the offset of the principal point in the calibration, for instance, he would be unable to judge whether the estimated image distortion model is appropriate or not.

Although the indexes (E) and (F) appear to be ideal indexes to evaluate an obtained image distortion model, a smaller value of the index (E) or (F) does not necessarily indicate that the obtained models is reliable. The dispersions of values of the indexes (E) and (F) in the cases of the inappropriate image distortion models were rather large as Figures 10 and 11 show. Therefore, calibration results by using different datasets in the simulation are necessary to evaluate the obtained image distortion model.

4. CONCLUSION

The results of the numerical simulation show the limits of capabilities of the indexes (A), (B) and (C) that are applied in order to evaluate calibration results in an ordinary camera calibration. The index (C) may be the most effective, however it is very difficult to interpret absolute values of the index (C) obtained in a camera calibration. A larger value of one of the indexes (A), (B) and (C) obtained in a camera calibration usually means that the image distortion model estimated by the calibration is not reasonable. On the other hand, smaller values of all of the indexes (A), (B) and (C) do not always mean that the estimated image distortion model is appropriate.

Moreover, the numerical simulation results indicate that an accurate image distortion model is not always necessary for the three-dimensional measurement if an orientation to estimate positions and attitudes of the camera is executed. It is obvious that an accurate image distortion model is required for the three-dimensional measurement with given positions and attitudes of the camera.

The authors propose that a set of the prior and posterior numerical simulations should be conducted in a camera calibration. The prior numerical simulation is carried out previous to image acquisition. The aim of the prior numerical simulation is to forecast precision of the camera calibration in progress. Image acquisition plan should be arranged according to the forecasted precision. The posterior numerical simulation based on the obtained calibration results is carried out to evaluate camera calibration results in addition to the conventional evaluation by using the indexes (A), (B) and (C) calculated at the estimation of camera parameters.

REFERENCES

Chikatsu, H., Nakano, K., Anai, T., Murai, S., 1996. CCD Camera Calibration for Real-time Photogrammetry. *Journal of the Japan Society of Photogrammetry and Remote Sensing*, Vol. 35, No. 2, pp. 20 - 25. (in Japanese)

Fraser, C. S., 2001. Photogrammetric Camera Component Calibration. *Calibration and Orientation of Cameras in Computer Vision*, A. Gruen and T. S. Huang Eds., Springer-Verlag, Berlin, pp. 95 - 121.

Fryer, J. G., 1996. Camera Calibration. *Close Range Photogrammetry and Machine Vision*, K.B. Atkinson Ed., Whittler Publishing, Caithness, pp. 156 - 179.

Habib, A. F., Shin S. W., Morgan M. F., 2002. New Approach for Calibrating Off-the-Shelf Digital Camera. *Proceedings of the ISPRS Commission III Symposium*, Part A, pp. 144 - 149.

Matsuoka, R., Fukue, K., Cho, K., Shimoda, H., Matsumae, Y., Hongo, K., Fujiwara, S., 2002. A Study on Calibration of Digital Camera. *Proceedings of the ISPRS Commission III Symposium*, Part B, pp. 176 - 180.

Murai, S., Matsuoka, R., Okuda, T., 1984. A Study on Analytical Calibration for Non Metric Camera and Accuracy of Three Dimensional Measurement. *International Archives of Photogrammetry and Remote Sensing*, Vol. XXV, Part B5, pp. 570 - 579.

Nasu, M., 1980. Self-Calibration of a Non-Metric Camera. *APA*, Vol. 11, No. 4, pp. 4 - 10. (in Japanese)

Noma, T., Otani, H., Ito, T., Yamada M., Kochi, N., 2002. New System of Digital Camera Calibration, DC-1000. *Proceedings of the ISPRS Commission V Symposium*, pp. 54 - 59.